Journal of

Materials Chemistry C

ARTICLE

Nonlinear optical chromophores containing novel pyrrole-based bridge: optimization of electro-optic activity and thermal stability by modifying the bridge

Fenggang Liu,[ab] Haoran Wang,[ab] Yuhui Yang,[ab] Huajun Xu,[ab] Maolin Zhang,[ab] Airui Zhang,[ab] Shuhui Bo,[a*] Zhen Zhen,[a] Xinhou Liu,[a] and Ling Qiu[a*]

Three novel second order nonlinear optical chromophores based on julolidinyl donors and tricyanovinyldihydrofuran (TCF) acceptors linked together via modified pyrrole π-conjugation (chromophores A and B) or thiophene moieties (chromophores C) as the bridges have been synthesized and systematically characterized. In particular, the pyrrole moiety as a bridge has been modified with the electron withdrawing groups (-Br, -NO₂) substituted benzene ring. The introduction of the side phenyl groups of chromophores A and B can increase the thermal, chemical stability and reduce dipole–dipole interactions so as to translate their hyperpolarizability (β) values into bulk EO performance more effectively than chromophore C. Moreover, DFT calculations suggested that the additional electron withdrawing groups in chromophores A and B could increase the β value than that of chromophores D without the substituted phenyl groups, and they showed different influences on the solvatochromic behavior, thermal stability, and electro-optic activity of the chromophores. EO responses (r₃₃values) of guest–host polymers containing pyrrole-bridged chromophores were reported. Incorporation of chromophores A and B into APC, provided large electro-optic coefficients of 86, 128 pm/V at 1310 nm with a high loading of 30 wt%. Film-C/APC containing 25wt% of chromophore C provides EO coefficient of 98 pm/V.

1. Introduction

In recent years, organic electro-optic (OEO) materials have attracted great attention owing to their potential applications in optical switches, optical sensors, information processors, and telecommunications etc. [1-3] Compared with inorganic materials, OEO materials have the potential advantages in lower cost, ease of processing, larger EO coefficients and so on. [4-6] To meet the stringent requirements for the using of devices, OEO materials should be developed through rational design of nonlinear optical (NLO) chromophores to optimize their first hyperpolarizability (β), and effectively translate these large β values into bulk EO activities together with improvement of other auxiliary properties like high thermal and chemical stability. [7]

The second-order NLO chromophores are based on a push-pull system, which consists of an electron-donating group (Donor) and an electron-withdrawing group (Acceptor) coupled through a π-conjugated bridge. [8, 9] Among the many types of NLO chromophores developed so far, strong electron donor and acceptor groups connected by a chemically, and thermally stable conjugated π-bridges have been widely employed. [10] Up to now, NLO chromophores containing bridges such as thiophene, [11, 12] locked phenyltetraene, [7] Azo, [13] phenyltetraene-based [14] have been reported. Among which thiophene and phenyltetraene bridges were wildly used. Further modification was wildly studied to achieve excellent and better performance. [14, 15] However, the pyrrole-based bridge, [16] the analogue of furan and thiophene moieties, has seldom been noticed, especially chromophores with a strong donor and a strong acceptor possibly due to its unstability. In fact, to the best of the authors' knowledge, few studies have reported on macroscopic EO response (r₃₃value) of poled films containing pyrrole-bridged chromophore. Practical applications of second-order NLO materials require thermally and chemically robust materials with a high electro-optic (EO) coefficient (r₃₃) value.

Above points prompted us to design and synthesize a series of pyrrole-bridged NLO chromophores with enhanced stability. Moreover, the β values of these chromophores can be effectively translated into large EO activities in poled polymers by suitable shape engineering. Modifications of the pyrrole-bridge have been explored for high electro-optic coefficient along with improved chemical and thermal stability to withstand encountered high temperatures in electric field poling and subsequent processing of chromophore/polymer materials. So that it can be applied to the electro-optic materials.

We used a strong julolidinyl-based donor,[17, 18] and tricyanovinyldihydrofuran (TCF) acceptor to construct our chromophores. In our syntheses, we found that when used as a bridge, the abundant electron density of the pyrrole makes it unstable. So, the labile nitrogen proton was replaced with aromatic blocks to improve stability. Moreover, a new method was proposed to introduce some electron-withdrawing units, which acted as an additional electron acceptor, to form a special type of organic chromophores. The additional electron acceptors (-Br, -NO$_2$) were substituted on the benzene ring so that the properties (like electron density) of the chromophore can be changed. The role of different auxiliary acceptor groups connected to the conjugated spacers of push–pull chromophores have been investigated and evaluated by theoretical methods. This introduced acceptor groups could not only increase the β values, but also reduce dipole–dipole interactions of these chromophores to improve EO activity.

reliable in predicting trends in hyperpolarizability,[19] and have been shown to predict experimental trends accurately.[20] Chromophore D without substituents of the pyrrole had not been synthesized due to its chemical and thermal unstability. However, the use of theoretical methods enables us to study the effects of structural modifications on optimizing of chromophore hyperpolarizability in this series of molecules.

2. Results and discussion

2.1 Synthesis and characterization of chromophores

Scheme 1 shows the synthetic approach for the new chromophores A, B, C. Starting from the amine donor aldehyde intermediates compound 3, chromophores A, B, C were synthesized in good overall yields through simple four main step reactions: The free hydroxyl group on the donors was protected by the alkyl group to improve the solubility through Williamson ether synthesis, after introduction of the bridge by Wittig condensation, compound 5a-c were prepared with a high yield. Treatment of compound 5a-b with POCl$_3$ and DMF gave an aldehyde 6a-b. Treatment of compound 5c with n-BuLi and DMF gave an aldehyde 6c. And the final condensations with the TCF acceptor give chromophores A, B, C all as green solids. All of the chromophores were fully characterized by ^{1}H-NMR, ^{13}C-NMR, elemental analysis and mass spectroscopy. These chromophores possess good solubility in common organic solvents, such as dichloromethane, chloromethane and acetone.
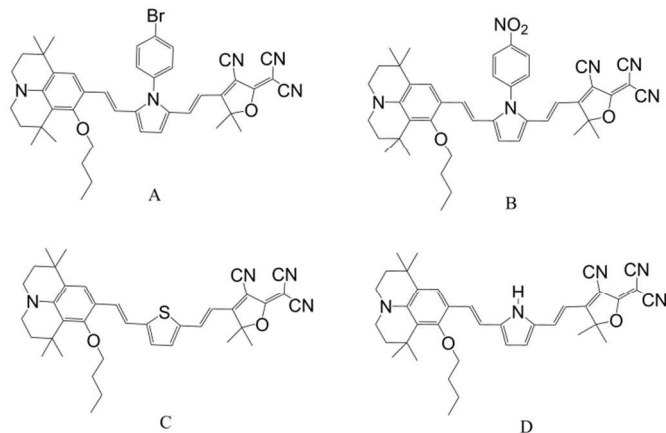

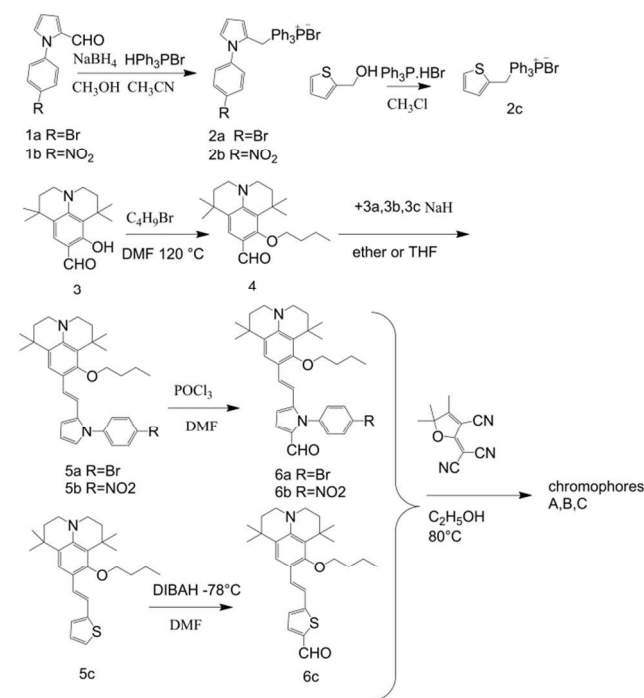Chart 1 Chemical structure for chromophores A, B, C, D.

In this study, we had designed and synthesized chromophores A, B based on modified pyrrole bridges. Chromophore C containing thiophene bridge had been synthesized for comparison (Chart 1). The UV-Vis, solvatochromic, redox properties, Density functional theory (DFT) quantum mechanical calculations, thermal stabilities and EO activities of these chromophores were systematically studied and compared to illustrate the influences of the modified bridges on rational NLO chromophore designs. Previous studies showed that the DFT method is considered

Scheme 1 Chemical structures and synthetic routes for chromophores A, B, C.

2.2 Thermal stability

The NLO chromophores must be thermally stable in order to withstand the poling process and subsequent processing for use. The thermal stability of the chromophores was investigated using thermo gravimetric analysis (TGA) and differential scanning calorimetry (DSC) as shown in Figure 1. Chromophores B and C appeared as highly crystalline compounds with a melting point at 196 °C and 198 °C, respectively, while chromophore A was obtained as an amorphous solid showing a glass transition temperature (T_g) at 190 °C. All the chromophores exhibited good thermal stabilities with the decomposition temperatures (T_d) higher than 200 °C (202 °C-251 °C). The chromophore A had the maximum decomposition temperature (T_d=251 °C). The chromophores A and B had higher decomposition temperature than that of chromophore C with thiophene bridge (T_d=202 °C). The enhanced thermal stability of chromophores A and B over chromophores C is due to the introduction of benzene ring into π-bridge pyrrole. While chromophores A and B had similar pyrrole bridge, they show different decomposition temperatures of 251 °C, 236 °C, respectively. This may due to the different properties of modified groups (-Br, -NO$_2$). The data indicate that the modified groups can influence the thermal stabilities of chromophores, thus we can modify the pyrrole bridge to improve thermal properties.
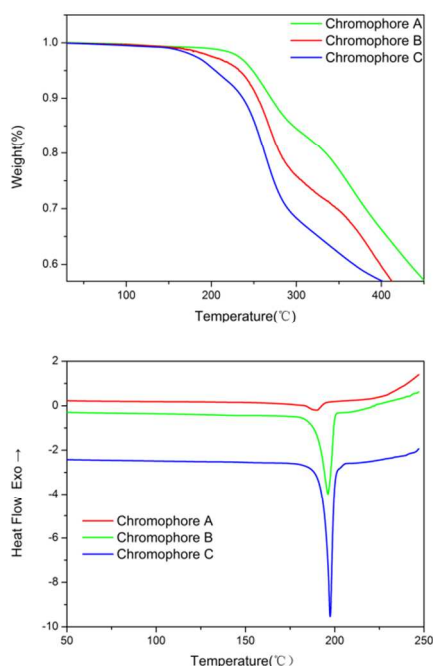

Fig. 1 TGA and DSC curves of chromophores A-C with a heating rate of 10 °C min^{-1} in nitrogen atmosphere.

2.3 Optical properties

To explore the different charge-transfer (CT) absorption properties of each chromophore, UV-Vis absorption spectra of three chromophores were measured in series solvents with different dielectric constants and in films, as shown in Figure 2. The spectra data are summarized in Table 1. It may see from the Figure 2 that chromophore A, B and C showed the maximum absorption (λ_{max}) from 723 nm to 728 nm in chloroform. Compared to chromophore C, chromophore A and B were slightly blue-shifted ($\Delta\lambda$=5nm, $\Delta\lambda$=3nm), and the two compounds containing pyrrole bridge exhibited similar charge-transfer band shape.
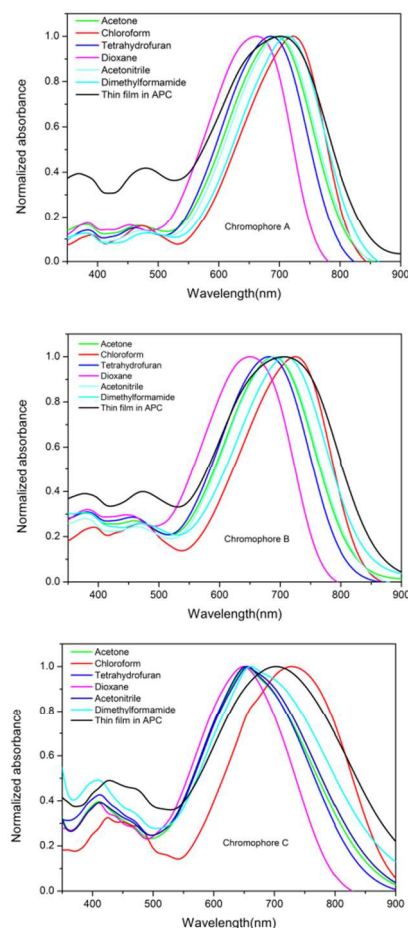
Fig. 2 UV-Vis absorption spectra of chromophore A, B and C in six kinds of aprotic solvents with varying dielectric constants (ε)

Besides, the solvatochromic behavior was also an important aspect to investigate the polarity of chromophores. It was found that both chromophores B and C showed very large bathochromic shifts of 79 nm, from dioxane to chloroform, displaying larger solvatochromism than that of CLD (60 nm) and the similar single donor FTC (61 nm) chromophore. [21, 22] While, chromophore A showed moderate bathochromic shift of

61 nm from dioxane to chloroform. This confirms that chromophores B and C are more easily polarizable than A although chromophore A had similar pyrrole bridge with chromophore B. [23] It is interesting to note that when continue to increase the dielectric constant of the solvent beyond chloroform, the NLO chromophore exhibited a negative solvatochromism. For example, compounds A and B showed hypsochromic shifts of -31nm and -36nm, respectively, from chloroform to acetone. Chromophore C also exhibited similar solvatochromic behavior. Such a phenomenon was reported by Davies [23] and was ascribed to the back electron transfer from the acceptor side to the donor side in polar solvents which causing blue-shift from the absorption. The same explanation should also hold for the present series of NLO chromophores.[24]

The photoluminescence emission spectra of A, B and C were also measured in different organic solvents. The spectra data are summarized in Table 1. Chromophore A, B and C showed Stokes Shifts of 137nm, 157nm, and 228nm in dioxane, and 130nm, 139nm, 223nm in chloroform respectively. Chromophore C showed larger Stokes Shifts than that of Chromophore A and B. Chromophore A showed the smallest Stokes Shifts.

2.4 Theoretical calculations and redox properties

The DFT calculations were carried out at the hybrid B3LYP level by employing the split valence 6-311g (d, p) basis set [25, 26] to understand the ground-state polarization of the chromophores with different bridges. When used carefully and consistently, this method of DFT has been shown to give relatively consistent descriptions of first-order hyperpolarizability for a number of similar chromophores.[7, 26] In order to compare the microscopic nonlinear effect between chromophores, the β value of chromophore D was also calculated. All molecules were assumed to be in trans-configurations. The HOMO-LUMO energy gaps, dipole moment (μ), and first hyperpolarizability (β) of the chromophores obtained from DFT calculations are summarized in Table 2.

For chromophore A and B, the additional electron acceptors (-Br, -NO$_2$) created another local dipole moment which result in larger total dipole moment than that of chromophore D. As reported earlier, the β value has a close relationship with the strength of the donor and acceptor end groups and on the nature and length of the bridge, substituents, steric hindrance and intramolecular charge-transfer and so on. [27, 28] Chromophore C showed the largest β value of all the four chromophores. This might be due to the molecular configuration and different combination effects among the donor, acceptor and bridge. The location of heterocyclic ring also plays critical role in determining β values, other than the nature of ring.[29] Pyrrole, being the most electron rich five-membered heteroaromatic ring may counteract the electron-withdrawing effect of the acceptor perhaps resulting in a decrease β value of chromophore A, B and D. [30]

Table 1 Optical Properties data of the Chromophores.

Chromophores	Ultraviolet spectrum				Fluorescence spectrum		
	λ_{max} [a] (nm)	λ_{max} [b] (nm)	$\Delta\lambda$ [c] (nm)	λ_{max} [d] (nm)	λ_{max} [e] (nm)	λ_{max} [f] (nm)	$\Delta\lambda$ [g] (nm)
A	662	723	61	702	799	853	54
B	646	725	79	706	803	864	61
C	649	728	79	703	877	951	74

[a]λ_{max} was measured in dioxane. [b]λ_{max} was measured in chloroform. [c]$\Delta\lambda$ was the difference between [a]λ_{max} and [b]λ_{max}. [d]λ_{max} was measured in films. [e]λ_{max} was measured in dioxane. [f]λ_{max} was measured in chloroform. [g]$\Delta\lambda$ was the difference between [e]λ_{max} and [f]λ_{max}.

Table 2 Summary of DFT and Electro-Chemical Data

Chromophore	$\Delta E(DFT)$ [a] (eV)	$\Delta E(CV)$ [b] (eV)	E_{ox} [c] (V)	E_{red} [d] (V)	μ [e] /D	β_{tot} [f] (10^{-30} esu)
A	2.02	1.36	0.12	-1.24	20.51	672.35
B	1.90	1.34	0.11	-1.23	21.62	686.10
C	1.96	1.35	0.09	-1.26	20.84	809.49
D	2.04	---	---	---	18.54	571.83

[a] $\Delta E(DFT)$ was calculated from DFT calculations. [b] $\Delta E(CV)$ was calculated from their corresponding oxidation and reduction potentials. [c] Referenced to ferrocene standard. [d] Referenced to ferrocene standard. μ [e] is the total dipole moment. β_{tot} [f] is the first-order hyperpolarizability, and where $\beta_{tot} = \sqrt{(\beta_x)^2 + (\beta_y)^2 + (\beta_z)^2}$ calculated from DFT quantum mechanical methods.

Optimization of the molecular first hyperpolarizability of dipolar EO chromophores relies on tuning of the electron density distribution through chemical modification of molecular constituents.[31] It may be noted, though having the similar pyrrole bridge, the β values of chromophore A and B were nearly 20% higher than that of chromophore D. This can be

explained that the abundant electron density of pyrrole ring would weaken by modified benzene ring groups which may led to increased β values. The additional electron acceptor incorporated into the conjugated system may facilitate the electron transfer from the donor to the acceptor, decreases the energy barrier of charge transfer transition which led to increased β value. From another perspective, the enhanced β values of chromophore A and B might be also ascribed to the fact that by adding an additional electron acceptor group perpendicular to the conjugated backbone could serve as an efficient spacer to reduce the formation of dipole couples. [15, 32] This may prove that the introduced special "auxiliary acceptor" group perpendicular to the conjugated backbone could increase the β values.

In order to determine the redox properties of chromophores A-C, cyclicvoltammetry (CV) measurements were conducted in degassed anhydrous acetonitrile solutions containing 0.1mol/L tetrabutylammonium hexafluorophosphate (TBAPF) as the supporting electrolyte. The relative data of 1×10^{-4} mol/L chromophore A-C were recorded, as shown in Table 2. The HOMO and LUMO levels of all three chromophores can be calculated from their corresponding oxidation and reduction potentials. [33] The difference between these two values provides the HOMO-LUMO energy difference ΔE (CV). The calculation results are summarized in Table 2. The HOMO levels of chromophore A-C were estimated to be -4.92, -4.91, and -4.89 eV, which showing a slight increase. In the meantime, the corresponding LUMO level of A-C only showed slight changes about -3.56, -3.57, and -3.54 eV, respectively. The HOMO-LUMO gap was the lowest for chromophore B (1.34 eV) and highest for chromophore A (1.36 eV). The narrower energy gap indicated easier charge transfer. [34, 35]

The HOMO-LUMO energy gaps ΔE (DFT) were also calculated by DFT calculations as shown in Table 2. The energy gaps between the HOMO and LUMO energy for chromophores A, B, C were 2.02, 1.90, and 1.96 eV. The electrochemical values are corroborated by the DFT calculations. Trends of energy gaps between ΔE (DFT) and ΔE (CV) for the chromophores were found to be consistent. As is commonly observed, ΔE (DFT) is significantly overestimated when compared to the data obtained by CV.
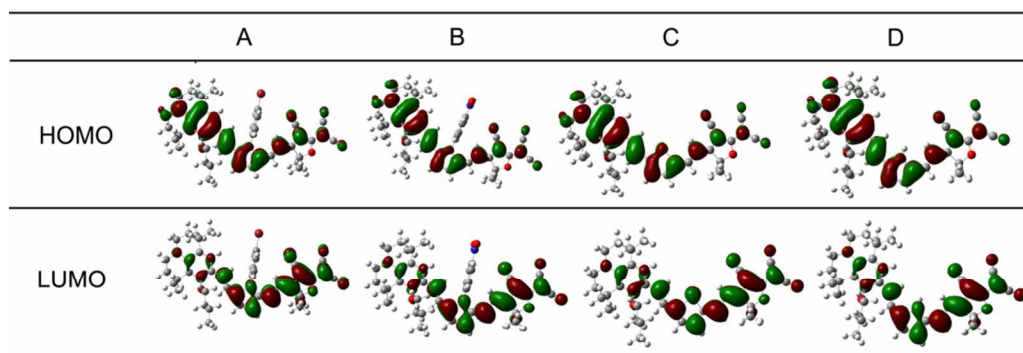

Fig. 3 The frontier molecular orbitals of chromophores A-D.

Table 3 The Molecular Orbital Composition (%) in the Ground State for Chromophores **A-D.**

Chromophore	**A**		**B**		**C**		**D**	
	HOMO	LUMO	HOMO	LUMO	HOMO	LUMO	HOMO	LUMO
donor	56.82%	16.28%	57.82%	16.39%	59.42%	16.79%	56.77%	16.22%
π bridge	25.02%	36.64%	24.57%	36.80%	25.44%	39.51%	24.75%	36.95%
acceptor	18.16%	47.08%	17.61%	46.81%	15.14%	43.70%	18.48%	46.83%

The molecular orbital composition was calculated using Multiwfn program with Ros-Schuit (SCPA) partition.

The frontier molecular orbitals are often used to obtain information about the optical and electrical properties of molecules. [34] Fig. 3 depicts the electron density distribution of the HOMO and LUMO structures which indicated the density of the ground and excited state electron is asymmetry along the dipolar axis of the chromophores.

To get more information from the frontier orbitals, the composition of the HOMOs and LUMOs has been calculated using the Multiwfn program. [36] The whole chromophore molecule was segmented as donor, π-bridge, and acceptor as shown in Table 3. For the chromophores A-D, the LUMO was largely stabilized by the contributions from acceptor (43.70%-47.08%) and the π-bridge (36.64%-39.51%), while the HOMO was largely stabilized by the contributions from donors (56.82%-59.42%) and π-bridge (24.57%-25.44%). The contribution of acceptor of chromophore A, B and D (46.81%-

47.08%) containing pyrrole-based bridge seemed to be bigger than that of chromophore C (43.70%) with thiophene-bridge for LUMO lever. As for HOMO level, the acceptor of chromophores A, B, D also contributed more than that of chromophore C.

2.5 Electro-Optic performance

The computational approach has helped to assess the relationship between bulk and molecular level non-linear optical (NLO) effects. For dipolar chromophores in an electric poling field, the electro-optic coefficient in the direction of the applied field is related to the molecular first hyperpolarizability by [37, 38]

$$r_{33} = \left| 2Nf(\omega)\beta \left\langle \cos^3 \theta \right\rangle / n^4 \right|$$

Where N is the chromophore number density (molecules/cm^3) in the polymer host, n is the index of refraction of the chromophore-containing polymeric material, and f (ω) is the product of local-field (Debye-Onsager) factors. $\cos^3$ (θ) is the acentric order parameter. θ is the angle between the permanent dipole moment of chromophores and the applied electric field. At low concentration, the electro-optic activity increased with chromophore density, dipole moment and the strength of electric poling field. However, when the concentrations of chromophores increased to a certain extent, the N and $\cos^3$ (θ) are no longer independent factor. Then,

$$< \cos^3 (\theta) > = \left(\mu F / 5kT \right) \left[1 - L^2 \left(W / kT \right) \right]$$

Where k is the Boltzmann constant and T is the Kelvin (poling) temperature. F= [f (0) E$_P$] where E$_p$ is the electric poling field. L is the Langevin function, which is a function of W/kT, the ratio of intermolecular electrostatic energy (W) to the thermal energy (kT). L is related to electrostatic interactions between molecules.
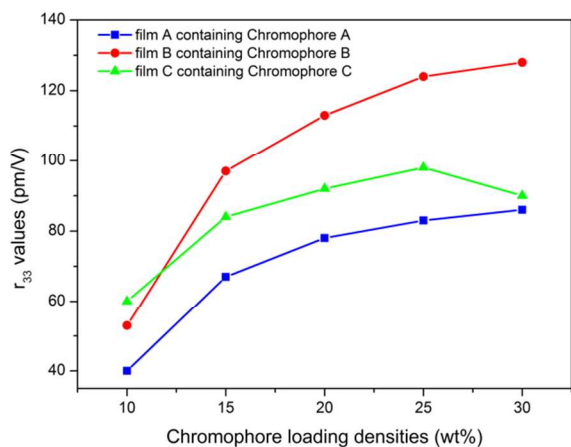

Fig. 4 r$_{33}$ values of NLO thin films as a function of chromophore loading densities.

This relationship succeeds in qualitatively predicting the important trends involving electro-optic activity although not the quantitative values of electro-optic coefficients. When the intermolecular electrostatic interactions are neglected, the electro-optic coefficient (r$_{33}$) should increase linearly with chromophore density, dipole moment, first hyperpolarizability and the strength of electric poling field. But chromophores with large dipole moment generate intermolecular static electric field dipole-dipole interaction, which leads to the unfavorable antiparallel packing of chromophores. So the number of truly oriented chromophore (N) is small. In molecular optimization, introducing the huge steric hindrance group to isolate chromophores is the most popular and easy way to attenuate the dipole-dipole interactions of chromophores. [39]
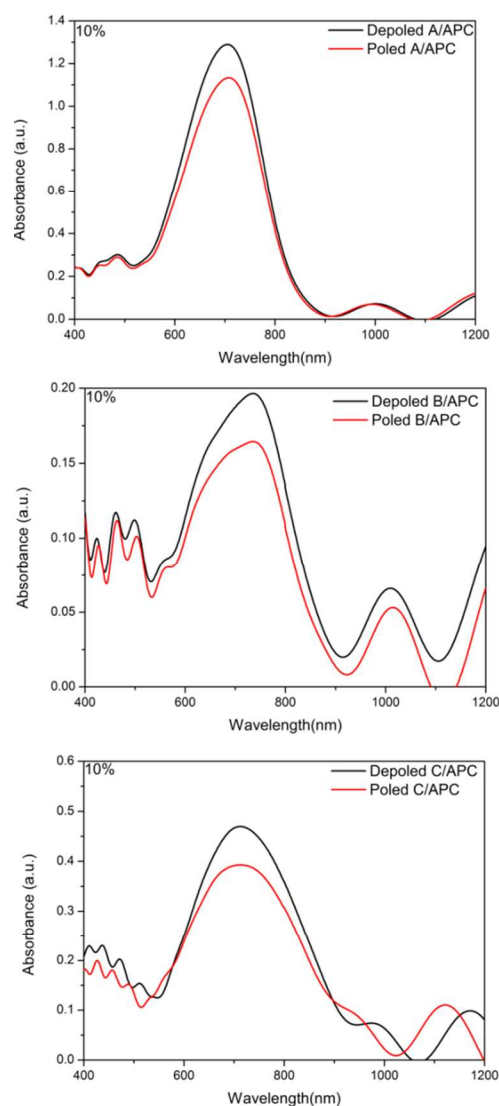

Fig. 5 UV-Vis absorption spectra of E-O polymers before and after poling (10%wt).

To achieve high EO coefficient, the chromophore should have facile intra charge transfer ability. The π-π stacking interactions and inter-molecular charge transport between chromophores should be reduced in order to translate the microscopic hyperpolarizability into macroscopic EO response more effectively. In order to balance the steric hindrance and the molecular free mobility for chromophore acentric alignment in guest host EO polymer, the poling condition should be carefully explored.[39]

In order to investigate the translation of the microscopic hyperpolarizability into macroscopic EO response, the polymer films doped with different concentrations of chromophores into amorphous polycarbonate (APC) were prepared using dibromomethane as solvent. The resulting solutions were filtered through a 0.2-μm PTFE filter and spin-coated onto indium tin oxide (ITO) glass substrates. Films of doped polymers were baked at 80 °C in a vacuum oven overnight. The corona poling process was carried out at a temperature of 10 °C above the glass transition temperature (T_g) of the polymer. The r_{33} values of poled films were measured by Teng–Man simple reflection method at a wavelength of 1310 nm using carefully selected thin ITO electrode with low reflectivity and good transparency in order to minimize the contribution from multiple reflections.[40, 41]

To evaluate their EO activities, 10 wt% of the chromophores A-C were doped into APC and formulated as the typical guest–host polymer. For this series of chromophores, the poled films of A/APC, B/APC and C/APC afforded r_{33} values of 40, 53 and 60 pmV^{-1}, respectively. To identify the underlying mechanism for the difference in achievable EO performance, the order parameter (Φ) was calculated by measuring UV-Vis absorption spectra. After the corona poling, the dipole moments of the chromophore moieties in the polymer were aligned, and the absorption curve decreased due to birefringence.[17] The order parameter (Φ) for films can be calculated from the absorption changes according to the following equation: $\Phi=1-A/A_0$,[42] in which A and A_0 are the respective absorptions of the polymer films after and before corona poling. The order parameter (Φ) of poled films was calculated. The Φ values of film-A/APC, B/APC, and C/APC are 12.12%, 16.28%, 16.34%, respectively as shown in Figure 5. The larger order parameters of film B, C indicate that film-B/APC, C/APC were more easily poled than film-A/APC. The film-C/APC achieved the largest r_{33} value probably due to its largest β and good polarizability. With relative lower β, the r_{33} value of film-B/APC was smaller than that of film-C/APC. The drop in EO activity from film-B/APC to film-A/APC is mainly associated with the lowest β of chromophore A in the polar polymer matrix and the inefficient poling, because of its less polarizable than the other two chromophores. This corresponded well with the results of solvatochromism study, DFT calculations and redox properties of chromophores.

The r_{33} values of film-A/APC, B/APC, and C/APC were measured in different loading densities, as shown in Fig.4. As a result, the r_{33} values of film-C/APC, were gradually improved from 60 pm/V (10 wt %) to 98 pm/V (25 wt %), while the r_{33}

values dropped to 90 pm/V as the loading density increasing from 25 wt % to 30 wt %. The r_{33} values of film-B/APC were improved from 53 pm/V (10 wt %) to 128 pm/V (30 wt %). The similar trend was also observed for film-A/APC whose r_{33} values increased from 40 pm/V (10 wt %) to 86 pm/V (30 wt %). When the concentration of chromophore in APC is low, film C/APC displayed a larger r_{33} value than that of the film B/APC. As the chromophore loading increased, this trend is inversed. This can be explained, when at a low-density range, the intermolecular dipolar interactions are relatively weak. The intermolecular dipole-dipole interactions would become stronger and stronger, accompanying with the increased concentration of NLO chromophore moieties in the polymer which would finally lead to a decreased NLO coefficient. The introduction of side-groups attached to the conjugated π-system can make inter-chromophore electrostatic interactions less favorable.[10, 43]
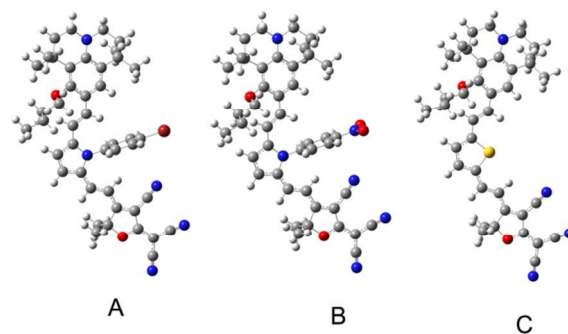

Fig. 6 The optimized structure of chromophore A, B and C.

The Φ values of film-A/APC, B/APC, and C/APC which containing 25 wt% of the chromophores are 18.02%, 20.38%, 17.26%, respectively. While the Φ values of film-A/APC, B/APC, and C/APC are 18.67%, 21.03%, 15.85%, respectively with a high loading of 30 wt% (see the ESI†). The difference in the order parameter indicates that film-A/APC, B/APC has weaker inter chromophore electrostatic interactions than film-C/APC in high density. It may be revealed by the optimized configurations (Fig.6) that the side benzene ring groups was perpendicular to the direction of the dipole moment of the chromophore which could act as the isolation group to suppress the possible aggregation. The film B/APC achieves the largest r_{33} value of 128 pm/V, even though it has relatively lower β. The high saturated loading density and lager Φ values of film-A, B were probably attributed to the fact that the chromophore structure isolated the chromophores from each other more effectively, thus improving the NLO effect at a higher chromophore loading density level.

Based on the above points, chromophores A and B containing modified pyrrole bridge can translate their large β values into bulk EO activities more effectively than chromophore C due to the isolation of modified benzene ring

groups. However, the different r_{33} values of film-A/APC and film B/APC, prove that the different auxiliary acceptor groups (-Br,-NO$_2$) showed different influences on molecular properties. Moreover, the large r_{33} values of the chromophores show that the modified pyrrole bridges were stable enough to withstand encountered high temperatures in electric field poling and subsequent processing of chromophore/polymer materials.

3. Conclusion

Three organic NLO chromophores with pyrrole or thiophene bridges had been synthesized and systematically characterized. The new chromophores obtained high thermal and chemical stabilities, large nonlinear optical coefficient, and good solubility in all common solvents. The pyrrole moiety as a bridge has been substituted with the modified phenyl groups. The introduction of the side phenyl groups helps to improve the chemical and thermal stability of unstable pyrrole moiety, so that it could be used in electro-optic (OEO) materials. Moreover the side groups can reduce dipole–dipole interactions so as to translate their hyperpolarizability (β) values into bulk EO performance more effectively than chromophore C. DFT calculations suggested the modified electron acceptor groups (-Br, -NO$_2$) in chromophores A and B could increase the β value, and they showed different influences on the solvatochromic behavior, thermal stability, and electro-optic activity of the chromophores. Incorporation of chromophores A and B into APC, provided large electro-optic coefficients of 86, 128 pm/V at 1310 nm with a high loading of 30 wt%. All these might be useful in designing other new NLO chromophores with modified pyrrole bridge to optimize molecular structure for achieving different properties. These novel modified pyrrole bridges will show promising applications in nonlinear optical (NLO) chromophore synthesis.

4. Experimental section

4.1 Materials and instrument

All chemicals are commercially available and are used without further purification unless otherwise stated. N, N-dimethyl formamide (DMF), Phosphorusoxychloride (POCl$_3$), tetrahydrofuran (THF) and ether was distilled over calcium hydride and stored over molecular sieves (pore size 3Å). 1-(4-bromophenyl)-1H-pyrrole-2-carbaldehyde (1a) was prepared according to the literature. [44] 1-(4-nitrophenyl)-1H-pyrrole-2-carbaldehyde (1b) was prepared according to the literature [45] The 2-dicyanomethylene-3-cyano-4-methyl-2,5-dihydrofuran(TCF) acceptor was prepared according to the literature. [37] Compound 2a, 2b was prepared according to the literature. [46] TLC analyses were carried out on 0.25 mm thick precoated silica plates and spots were visualized under UV light. Chromatography on silica gel was carried out on Kieselgel (200-300 mesh).

4.2 Measurements and instrumentation

^{1}HNMR spectra were determined by an Advance Bruker 400M (400 MHz) NMR spectrometer (tetramethylsilane as internalreference). The MS spectra were obtained on MALDI-TOF (Matrix Assisted Laser Desorption/Ionization of Flight) on BIFLEXIII (Broker Inc.) spectrometer. The UV-Vis spectra were performed on Cary 5000 photo spectrometer. The TGA was determined by TA5000-2950TGA (TA co) with a heating rate of 10 °C min^{-1} under the protection of nitrogen. Cyclic voltammetric data were measured on a BAS CV-50W voltammetric analyzer using a conventional three-electrode cell with Pt metal as the working electrode, Pt gauze as the counter-electrode, and Ag/AgNO$_3$ as the reference electrode at a scan rate of 50 mV s^{-1}. The 0.1 M tetrabutylammonium hexa-fluorophosphate (TBAPF) in acetonitrile is the electrolyte. The fluorescence spectra were performed on Hitachi F-4500 fluorescence spectrometers. The elemental analysis was measured on Flash EA 1112 Elemental Analyzer. The melt points were obtained by TA DSC Q10 under N$_2$ at a heating rate of 10 °C min^{-1}.

4.3 Synthesis and characterization

Compound 4

Under a N$_2$ atmosphere, anhydrous potassium carbonate (6.4 g, 40 mmol) was added to a solution of compound 3 (5.46 g, 20 mmol) and compound C$_4$H$_9$Br (4.11 g, 30 mmol) in DMF (120 mL). The mixture was allowed to stir at 120 ºC for 12 h and then poured into water. The organic phase was extracted by AcOEt, washed with brine and dried over MgSO$_4$. After removal of the solvent under reduced pressure, the crude product was purified by silica chromatography, eluting with (Acetone: Hexane=1:10) to give compound 4 as a yellow powder with 91.3% yield (6.02 g, 18.26 mmol). ^{1}H NMR (400 MHz, Acetone) δ 9.90 (1H, s, CHO), 7.48 (1H, s, ArH), 3.96 (2H, t, J = 6.8 Hz, OCH$_2$), 3.36 − 3.33 (2H, m, NCH$_2$), 3.30 − 3.26 (2H, m, NCH$_2$), 1.86 (2H, dd, J = 14.9, 7.0 Hz, CH$_2$), 1.76 − 1.66 (4H, m, CH$_2$), 1.52 (2H, dt, J = 14.8, 7.5 Hz, CH$_2$), 1.41 (6H, s, CH$_3$), 1.23 (6H, s, CH$_3$), 0.99 (3H, t, J = 7.4 Hz, CH$_3$); MS (EI) (M$^+$, C$_{21}$H$_{31}$NO$_2$): calcd: 329.4837; found: 329.2485. m.p. : 223.83 ºC

Compound 5a

Under a N$_2$ atmosphere, to a solution of compound 4 (0.99 g, 3 mmol) and 3a (2.08 g, 3.6 mmol) in ether (100 mL) was added NaH (0.43 g, 18 mmol). The solution was allowed to stir for 48h and then poured into water. The organic phase was extracted by AcOEt, washed with brine and dried over MgSO$_4$. After removal of the solvent under reduced pressure, the crude product was purified by silica chromatography, eluting with (Acetone: Hexane = 1:20) to give compound 5a as orange oil with 83.7% yield (1.37 g, 2.51 mmol). ^{1}H NMR (400 MHz, Acetone) δ 7.60 (2H, d, J = 6.6Hz, ArH), 7.38 (1H，d, J = 8.7 Hz, CH), 7.23 (2H, d, J = 6.6 Hz, ArH), 7.08 (1H，s, ArH), 6.87 (1H, d, J = 8.7, CH), 6.32 (1H, d, J = 11.9 Hz, PrH), 6.23

– 6.18 (1H, m, PrH), 6.11 (1H, d, J = 11.9 Hz, PrH), 3.61 (2H, t, J = 6.7 Hz, OCH$_2$), 3.13 – 3.09 (2H，m, NCH$_2$), 3.08 – 3.02 (1H，m, NCH$_2$), 1.70 (6H，m, CH$_2$), 1.52 – 1.42 (2H, m, CH$_2$), 1.36 (6H，s, CH$_3$), 1.10 (6H，s, CH$_3$), 0.95 (3H, t, J = 7.3 Hz, CH$_3$); MS (MALDI) (M+, C$_{32}$H$_{39}$BrN$_2$O): calcd: 547.573; found: 547.258.

Compound 5b

The procedure for compound 5a was followed to prepare 5b from 4 and 3b as red oil with 56.7% yield (0.87 g, 1.71 mmol). ^{1}H NMR (400 MHz, Acetone) δ 8.40 (2H，d, J = 9.9 Hz, ArH), 7.71 (2H, d, J =9.9 Hz, ArH), 7.17 (1H ,s, PrH), 7.08 (1H, s, ArH), 7.01 (1H, d, J = 16.2 Hz, CH), 6.69 (1H, d, J = 16.2 Hz, CH=), 6.58 (1H, d, J = 3.4 Hz, PrH), 6.34 (1H, t, J = 3.4 Hz, PrH), 3.83 (2H, t, J = 6.6 Hz, OCH$_2$), 3.16 – 3.11 (2H, m, NCH$_2$), 3.10 – 3.05 (2H, m, NCH$_2$), 1.77 (2H, dd, J = 14.5, 7.4 Hz, CH$_2$), 1.73 – 1.65 (4H, m, CH$_2$), 1.51 (2H, dd, J = 15.1, 7.4 Hz, CH$_2$), 1.39 (6H, s, CH$_3$), 1.18 (6H, s, CH$_3$), 0.96 (3H, t, J = 7.4 Hz, CH$_3$); MS (MALDI): m/ z (M+, C$_{32}$H$_{39}$N$_3$O$_3$): calcd: 513.073; found: 513.098.

Compound 5c

The procedure for compound 5a was followed to prepare 5c from 4 and 3c as orange oil in 86.3% yield (1.06 g, 2.59 mmol). The ratio of the Z: E isomer is 50: 50% calculated by the integration of respective protons. ^{1}H NMR (400 MHz, CDCl$_3$) δ 7.16 (1H, m, PrH), 7.09 (1H, d, J = 5.0 Hz, PrH), 7.07 (1H, d, J = 5.0 Hz, PrH), 7.04 (0.5H, d, J = 3.4 Hz, CH), 6.98 (1H, s, ArH), 6.91 (1H, d, J = 3.6 Hz, CH), 6.57 (0.5H, d, J = 11.8 Hz, CH), 6.48 (0.5H, d, J = 11.8 Hz, CH$_2$), 3.89 (2H, m, OCH$_2$), 3.19 – 3.13 (2H, m, NCH$_2$), 3.13 – 3.05 (2H, m, NCH$_2$), 1.93 – 1.80 (2H, m, CH$_2$), 1.80 – 1.71 (4H, m, CH$_2$), 1.58 (3H, m, CH$_2$), 1.44 (3H, s, CH$_3$), 1.43 (3H, s, CH$_3$), 1.31 (3H, s, CH$_3$), 1.17 (3H, s, CH$_3$), 1.01 (1.5H, t, J = 7.4 Hz, CH$_3$), 0.94 (1.5H, t, J = 7.4 Hz, CH$_3$); MS (MALDI) (M$^+$, C$_{26}$H$_{35}$NOS): calcd: 410.045; found: 410.033

Compound 6a

 DMF (0.42 g, 5.75 mmol) was added to freshly distilled POCl$_3$ (0.59 g, 3.84 mmol) under an atmosphere of N$_2$ nitrogen at 0 °C, and the resultant solution was stirred until its complete conversion into a glassy solid. After the addition of 5a (1.40 g, 2.56 mmol) in 1,2-dichloroethane (60 mL) dropwise, the mixture was stirred at room temperature overnight, then poured into an saturation aqueous solution of sodiumacetate (300 mL). After 2 hour stirring at room temperature, the mixture extracted with chloroform (5 × 30 mL), and the organic fractions were collected and dried over anhydrous MgSO$_4$. The crude product was purified through a silica gel chromatography eluting with (Acetone: Hexane = 1:5) to afford a red solid 6a with 73.2% yield (1.08 g, 1.87mmol). ^{1}H NMR (400 MHz, Acetone) δ 9.38 (1H, s, CHO), 7.71 (2H，d, J = 8.4 Hz, ArH), 7.33 (2H, d, J = 8.4 Hz, ArH), 7.26 (1H, d, J = 16.3 Hz, CH), 7.14 (1H, d, J =

4.2 Hz, PrH), 7.05 (1H, s, ArH), 6.73 (1H, d, J = 4.2 Hz, PrH), 6.39 (1H, d, J = 16.3 Hz, CH), 3.78 (2H, t, J = 6.7 Hz, OCH$_2$), 3.19 – 3.14 (2H, m, NCH$_2$), 3.13 – 3.07 (2H, m, NCH$_2$), 1.76 (2H, dd, J = 14.3, 7.2 Hz, CH$_2$), 1.72 – 1.64 (4H, m, CH$_2$), 1.52 (2H, dd, J = 14.3, 7.2 Hz, CH$_2$), 1.38 (6H, s, CH$_3$), 1.15 (6H, s, CH$_3$), 0.99 (3H, t, J = 7.3 Hz, CH$_3$); ^{13}C NMR (101 MHz, Acetone) δ 176.77, 156.37, 143.58, 142.74, 136.97, 133.39, 132.16, 130.55, 129.92, 126.37, 123.36, 122.04, 117.58, 110.78, 106.66, 74.45, 47.09, 46.29, 40.37, 36.64, 32.60, 32.18, 32.02, 30.70, 29.95, 19.43, 13.77; MS (MALDI) (M$^+$, C$_{33}$H$_{39}$BrN$_2$O$_2$): calcd: 575.867; found: 575.957.

Compound 6b

The procedure for compound 6a was followed to prepare 6b from 5b as red solid in 71.8% yield (0.99 g, 1.84 mmol). ^{1}H NMR (400 MHz, Acetone) δ 9.44 (1H, s, CHO), 8.43 (2H，d, J = 8.9 Hz, ArH), 7.69 (2H, d, J = 8.9 Hz, ArH), 7.32 (1H, d, J = 16.2 Hz, CH), 7.24 (1H, d, J = 4.2 Hz, PyH), 7.07 (1H, s, ArH), 6.81 (1H, d, J = 4.2 Hz, PyH), 6.41 (1H, d, J = 16.2 Hz, CH), 3.79 (2H, t, J = 6.7 Hz, NCH$_2$), 3.79 (2H, t, OCH$_2$), 3.18(2H, t, NCH$_2$),3.13(2H, t, NCH$_2$), 1.79 – 1.73 (2H, m, CH$_2$), 1.72 – 1.63 (4H, m, CH$_2$), 1.52 (2H, m, 7.6 Hz, CH$_2$), 1.38 (6H, s, CH$_3$), 1.14 (6H, s, CH$_3$), 0.99 (3H, t, CH$_3$); ^{13}C NMR (101 MHz, CDCl$_3$) δ 176.77, 156.33, 147.21, 143.66, 143.09, 132.30, 131.18, 129.17, 124.01, 122.53, 109.34, 107.36, 74.77, 47.20, 46.68, 39.87, 36.10, 32.51, 32.07, 31.95, 30.77, 29.93, 19.28, 13.90; MS (MALDI) (M$^+$, C$_{33}$H$_{39}$N$_3$O$_4$): calcd: 541.136; found: 541.138.

Compound 6c

Under a N$_2$ atmosphere, 5c (0.41 g, 1 mmol) was dissolved in 150 mL of freshly distilled THF and cooled to -78 °C. Approximately 2 equivalents of BuLi in hexanes (20 mL, 5 mmol) was added drop wise over 20 min. Reaction continued at -78 °C for 1 h at which time DMF (0.37 g, 5 mol) was added over 1 min. The reaction was allowed to reach RT while the solution stirred for 1h. The organic phase was extracted by AcOEt, washed with brine and dried over MgSO$_4$. After removal of the solvent under reduced pressure, the crude product was purified by silica chromatography, eluting with (Acetone: Hexane = 1:5) to give compound 6c as an orange oil with 75.6% yield (0.33 g, 0.76 mmol). ^{1}H NMR (400 MHz, CDCl$_3$) δ 9.82 (1H, s, CHO), 7.64 (1H d, J = 3.9 Hz,CH), 7.33 (1H，d, J = 16.1 Hz, CH), 7.27 (1H, d, J = 5.9 Hz, CH), 7.05 (1H, d, J = 5.9 Hz, CH), 6.96 (1H,d, J = 16.1 Hz, CH), 3.84 (2H,t, J = 6.7 Hz, OCH$_2$), 3.23 – 3.19 (2H,m, NCH$_2$), 3.16 – 3.12 (2H, m, CH$_2$), 1.91 – 1.83 (2H, m, CH$_2$), 1.77 – 1.72 (4H, m, CH$_2$), 1.60 – 1.53 (2H, m, CH$_2$), 1.43 (6H, s, CH$_3$), 1.31 (6H, s, CH$_3$), 1.01 (3H, t, J = 7.3 Hz, CH$_3$); ^{13}C NMR (101 MHz, CDCl$_3$) δ 181.23, 155.85, 153.99, 138.83, 136.30, 121.99, 123.33, 121.32, 114.32, 66.95, 46.41, 45.74, 39.11, 35.43, 31.70, 31.27, 30.14, 29.88, 29.02 28.68, 24.50, 21.53, 18.54, 13.10; MS (MALDI) (M$^+$, C$_{27}$H$_{35}$NO$_2$S): calcd: 437.347; found: 437.181

Chromophore A

To a solution of 6a (0.29 g, 0.50mmol) and the TCF acceptor (0.12 g, 0.60 mmol) in MeOH (60 mL) was added several drops of triethyl amine. The reaction was allowed to stir at 78 ºC for 5 h. The reaction mixture was cooled and green crystal precipitation was facilitated. After removal of the solvent under reduced pressure, the crude product was purified by silica chromatography, eluting with (AcOEt: Hexane = 1:5) to give chromophore A as a green solid in 32.3% yield (0.12 g, 0.16 mmol). ^{1}H NMR (400 MHz, Acetone) δ 8.11 (1H, d, J = 15.6 Hz, CH), 7.62 (2H, d, J = 9.5 Hz, ArH), 7.36 (2H, d, J = 9.5 Hz, ArH), 7.22 (1H, s, ArH), 7.05 (1H, d, J = 3.3 Hz, PyH), 6.90 (1H, d, J = 3.3 Hz, PyH), 6.83 (1H, d, J = 15.6 Hz, CH), 6.76 (2H, s, CH), 3.62 (2H, t, J = 6.6 Hz, OCH$_2$), 3.15 – 3.09 (2H, m, NCH$_2$), 3.08 – 3.02 (2H, m, NCH$_2$), 1.67 (6H, s, CH$_3$), 1.58 (6H, m, CH$_2$), 1.53 – 1.44 (2H, m, CH$_2$), 1.26 (6H, s, CH$_3$), 1.10 (6H, s, CH$_3$), 0.76 (3H, t, J = 8.5 Hz, CH$_3$); ^{13}C NMR (101 MHz, Acetone) δ 175.06, 156.38, 143.69, 141.90, 140.50, 137.93, 133.55, 132.25, 126.65, 126.65, 122.63, 121.75, 121.39, 120.81, 116.84, 112.30, 111.55, 111.26, 109.93, 109.08, 107.86, 97.03, 92.50, 74.17, 53.50, 52.28, 46.44, 45.91, 39.63, 35.84, 31.96, 31.47, 29.91, 25.05, 18.57, 12.98; MS (MALDI) (M$^+$, C$_{44}$H$_{46}$BrN$_5$O$_2$): calcd: 756.776; found: 756.686. m.p. : 189.48 ºC. Anal. Calcd (%) for C$_{44}$H$_{46}$BrN$_5$O$_2$: C, 69.83; H, 6.13; N, 9.25; found: C, 70.03; H, 6.17; N, 9.22;

Chromophore B

The procedure for chromophore A was followed to prepare chromophore B from 6b as a green solid in 33.9% yield (0.12 g, 0.17 mmol). The ratio of the Z: E isomers were 50:50% calculated by the integration of respective protons. ^{1}H NMR (400 MHz, Acetone) δ 8.57 (1H, d, J = 8.9 Hz, ArH), 8.44 (1H, d, J = 6.9 Hz, ArH), 8.22 (0.5H, d, J = 15.7 Hz, CH), 7.85 (2H, d, J = 8.9 Hz, ArH), 7.69 (0.5H, d, J = 4.6 Hz, CH), 7.60 (0.5H, d, J = 15.4 Hz, CH), 7.47 (0.5H, d, J = 16.1 Hz, CH), 7.38 (0.5H, s, PrH), 7.33 (0.5H, d, J = 3.4 Hz, CH), 7.14 (0.5H, s, PrH), 7.12 (0.5H, d, J = 4.7 Hz, CH), 7.11 (0.5H, d, J = 3.4 Hz, CH), 7.01 (0.5H, d, J = 15.7 Hz, CH), 6.95 (1H, s, ArH), 6.63 (0.5H, d, J = 15.4 Hz, CH), 6.55 (0.5H, d, J = 16.1 Hz, CH), 3.78 (2H, dd, J = 11.9, 6.6 Hz, OCH$_2$), 3.27 – 3.22 (2H, m, NCH$_2$), 3.18 (2H, dd, J = 5.9, 4.5 Hz, NCH$_2$), 1.81 (3H, s, CH$_3$), 1.77 – 1.64 (6H, m, CH$_2$), 1.64 (3H, s, CH$_3$), 1.51 (2H, m, CH$_2$), 1.38 (6H, s, CH$_3$), 1.22 (3H, s, CH$_3$), 1.14 (3H, s, CH$_3$), 0.98 (1.5H, t, J = 7.4 Hz, CH$_3$), 0.87 (1.5H, t, J = 7.4 Hz, CH$_3$); ^{13}C NMR (101 MHz, Acetone) δ 176.35, 156.68, 146.30, 143.99, 141.73, 140.94, 134.07, 133.36, 132.59, 132.16, 129.84, 125.91, 124.83, 124.54, 123.18, 122.70, 121.77, 121.59, 121.57, 116.46, 111.42, 109.07, 106.94, 97.24, 96.35, 74.31, 64.49, 46.46, 45.90, 39.43, 35.69, 31.94, 31.54, 31.35, 29.87, 29.61, 24.85, 18.73, 13.00; MS (MALDI) (M$^+$, C$_{44}$H$_{46}$N$_6$O$_4$): calcd: 722.878 found: 722.902. m.p. : 195.98 ºC. Anal. Calcd (%) for C$_{44}$H$_{46}$N$_6$O$_4$: C, 73.11; H, 6.41; N, 11.63; found: C, 73.20; H, 6.43; N, 11.67;

Chromophore C

The procedure for chromophore A was followed to prepare chromophore C from 6c as a green solid in 68.9% yield (0.21 g, 0.34 mmol). ^{1}H NMR (400 MHz, CDCl$_3$) δ 7.73 (1H，d, J = 15.5 Hz, CH), 7.31 (1H,d, J = 4.0 Hz, CH), 7.26 (1H, d, J = 15.9 Hz, CH), 7.19 (1H, s, ArH), 6.96 (1H, d, J = 4.0 Hz, CH), 6.92 (1H, d, J = 15.9 Hz, CH), 6.44 (1H, d, J = 15.5 Hz, CH), 3.78 (2H, t, J = 6.7 Hz, OCH$_2$), 3.22 – 3.15 (2H, m, NCH$_2$), 3.14 – 3.07 (2H, m, NCH$_2$), 1.67 (6H, s, CH$_3$), 1.57 – 1.46 (8H, m, CH$_2$), 1.24 (6H ,s, CH$_3$), 1.19 (6H, s, CH$_3$), 0.96 (3H, t, J = 7.4 Hz, CH$_3$); ^{13}C NMR (101 MHz, CDCl$_3$) δ 174.88, 171.68, 154.84, 154.83, 154.68, 138.30, 136.77, 136.10, 130.76, 126.29, 126.27, 125.61, 122.13, 114.58, 110.25, 110.16, 110.11, 95.80, 94.39, 74.74, 54.46, 46.61, 46.09, 38.73, 35.00, 31.72, 31.26, 29.90, 28.34, 25.53, 18.59, 13.09; MS (MALDI) (M$^+$, C$_{38}$H$_{42}$N$_4$O$_2$S): calcd: 618.186; found: 618.204. m.p. : 197.56 ºC Anal. Calcd (%) for C$_{38}$H$_{42}$N$_4$O$_2$S : C, 73.75; H, 6.84; N, 9.05; found: C, 73.83; H, 6.90; N, 9.02;

Notes and references

a Key Laboratory of Photochemical Conversion and Optoelectronic Materials, Technical Institute of Physics and Chemistry, Chinese Academy of Sciences, Beijing 100190, PR China

b University of Chinese Academy of Sciences, Beijing 100043, PR China

* Corresponding authors. Tel.: +86-01-82543529; Fax: +86-01-2543529

E-mail address: boshuhui@mail.ipc.ac.cn (S. Bo), qiuling@mail.ipc.ac.cn

1. J. Y. Lee, H. B. Bang, T. S. Kang and E. J. Park, *Eur. Polym. J.*, 2004, 40, 1815-1822.
2. B. J. Coe, S. P. Foxon, E. C. Harper, M. Helliwell, J. Raftery, C. A. Swanson, B. S. Brunschwig, K. Clays, E. Franz, J. Garin, J. Orduna, P. N. Horton and M. B. Hursthouse, *J. Am. Chem. Soc.*, 2010, 132, 1706-1723.
3. I. Fuks-Janczarek, J. M. Nunzi, B. Sahraoui, I. V. Kityk, J. Berdowski, A. M. Caminade, J. P. Majoral, A. C. Martineau, P. Frere and J. Roncali, *Opt. Commun.*, 2002, 209, 461-466.
4. H. Y. Li and F. Jakle, *Macromol. Rapid Commun.*, 2010, 31, 915-920.
5. K. H. Park, J. T. Lim, S. Song, Y. S. Lee, C. J. Lee and N. Kim, *React. Funct. Polym.*, 1999, 40, 177-184.
6. S. W. Wang, L. S. Zhao, X. L. Zhang, X. Zhang, Z. S. Shi, Z. C. Cui, X. Chen and Y. Q. Yang, *Polym. Int.*, 2009, 58, 933-938.
7. X. H. Zhou, J. Davies, S. Huang, J. D. Luo, Z. W. Shi, B. Polishak, Y. J. Cheng, T. D. Kim, L. Johnson and A. Jen, *J. Mater. Chem.*, 2011, 21, 4437-4444.
8. F. Dumur, C. R. Mayer, E. Dumas, F. Miomandre, M. Frigoli and F. Secheresse, *Org. Lett.*, 2008, 10, 321-324.
9. R. M. El-Shishtawy, F. Borbone, Z. M. Al-Amshany, A. Tuzi, A. Barsella, A. M. Asiri and A. Roviello, *Dyes Pigment.*, 2013, 96, 45-51.
10. D. Briers, L. De Cremer, G. Koeckelberghs, S. Foerier, T. Verbiest and C. Samyn, *Macromol. Rapid Commun.*, 2007, 28, 942-947.

11. J. M. Raimundo, P. Blanchard, P. Frere, N. Mercier, I. Ledoux-Rak, R. Hierle and J. Roncali, *Tetrahedron Lett.*, 2001, 42, 1507-1510.
12. S. R. Hammond, O. Clot, K. A. Firestone, D. H. Bale, D. Lao, M. Haller, G. D. Phelan, B. Carlson, A. K. Y. Jen, P. J. Reid and L. R. Dalton, *Chem. Mat.*, 2008, 20, 3425-3434.
13. Y. Q. Zhang, J. Ortega, U. Baumeister, C. L. Folcia, G. Sanz-Enguita, C. Walker, S. Rodriguez-Conde, J. Etxebarria, M. J. O'Callaghan and K. More, *J. Am. Chem. Soc.*, 2012, 134, 16298-16306.
14. J. D. Luo, S. Huang, Y. J. Cheng, T. D. Kim, Z. W. Shi, X. H. Zhou and A. K. Y. Jen, *Org. Lett.*, 2007, 9, 4471-4474.
15. Y. J. Cheng, J. D. Luo, S. Huang, X. H. Zhou, Z. W. Shi, T. D. Kim, D. H. Bale, S. Takahashi, A. Yick, B. M. Polishak, S. H. Jang, L. R. Dalton, P. J. Reid, W. H. Steier and A. K. Y. Jen, *Chem. Mat.*, 2008, 20, 5047-5054.
16. Q. Q. Li, C. G. Lu, J. Zhu, E. Fu, C. Zhong, S. Y. Li, Y. P. Cui, J. G. Qin and Z. Li, *J. Phys. Chem. B*, 2008, 112, 4545-4551.
17. J. Y. Wu, J. L. Liu, T. T. Zhou, S. H. Bo, L. Qiu, Z. Zhen and X. H. Liu, *RSC Adv.*, 2012, 2, 1416-1423.
18. X. H. Zhou, J. D. Luo, J. A. Davies, S. Huang and A. K. Y. Jen, *J. Mater. Chem.*, 2012, 22, 16390-16398.
19. J. B. Wu, B. A. Wilson, D. W. Smith and S. O. Nielsen, *J. Mater. Chem. C*, 2014, 2, 2591-2599.
20. P. A. Sullivan and L. R. Dalton, *Accounts Chem. Res.*, 2010, 43, 10-18.
21. C. Zhang, L. R. Dalton, M. C. Oh, H. Zhang and W. H. Steier, *Chem. Mat.*, 2001, 13, 3043-3050.
22. X. Q. Piao, X. M. Zhang, S. Inoue, S. Yokoyama, I. Aoki, H. Miki, A. Otomo and H. Tazawa, *Org. Electron.*, 2011, 12, 1093-1097.
23. J. A. Davies, A. Elangovan, P. A. Sullivan, B. C. Olbricht, D. H. Bale, T. R. Ewy, C. M. Isborn, B. E. Eichinger, B. H. Robinson, P. J. Reid, X. Li and L. R. Dalton, *J. Am. Chem. Soc.*, 2008, 130, 10565-10575.
24. X. H. Ma, F. Ma, Z. H. Zhao, N. H. Song and J. P. Zhang, *J. Mater. Chem.*, 2010, 20, 2369-2380.
25. C. Lee and R. G. Parr, *Phys. Rev. A*, 1990, 42, 193-200.
26. C. M. Isborn, A. Leclercq, F. D. Vila, L. R. Dalton, J. L. Bredas, B. E. Eichinger and B. H. Robinson, *J. Phys. Chem. A*, 2007, 111, 1319-1327.
27. L. T. Cheng, W. Tam, S. H. Stevenson, G. R. Meredith, G. Rikken and S. R. Marder, *J. Phys. Chem.*, 1991, 95, 10631-10643.
28. L. T. Cheng, W. Tam, S. R. Marder, A. E. Stiegman, G. Rikken and C. W. Spangler, *J. Phys. Chem.*, 1991, 95, 10643-10652.
29. P. R. Varanasi, A. K. Y. Jen, J. Chandrasekhar, I. N. N. Namboothiri and A. Rathna, *J. Am. Chem. Soc.*, 1996, 118, 12443-12448.
30. M. M. M. Raposo, A. Sousa, G. Kirsch, P. Cardoso, M. Belsley, E. D. Gomes and A. M. C. Fonseca, *Org. Lett.*, 2006, 8, 3681-3684.
31. L. R. Dalton, P. A. Sullivan and D. H. Bale, *Chem. Rev.*, 2010, 110, 25-55.
32. I. Liakatas, C. Cai, M. Bosch, M. Jager, C. Bosshard, P. Gunter, C. Zhang and L. R. Dalton, *Appl. Phys. Lett.*, 2000, 76, 1368-1370.
33. M. Thelakkat and H. W. Schmidt, *Adv. Mater.*, 1998, 10, 219-+.
34. R. M. Ma, P. Guo, L. L. Yang, L. S. Guo, X. X. Zhang, M. K. Nazeeruddin and M. Gratzel, *J. Phys. Chem. A*, 2010, 114, 1973-1979.
35. H. J. Xu, M. L. Zhang, A. R. Zhang, G. W. Deng, P. Si, H. Y. Huang, C. C. Peng, M. K. Fu, J. L. Liu, L. Qiu, Z. Zhen, S. H. Bo and X. H. Liu, *Dyes Pigment.*, 2014, 102, 142-149.
36. R. V. Solomon, P. Veerapandian, S. A. Vedha and P. Venuvanalingam, *J. Phys. Chem. A*, 2012, 116, 4667-4677.
37. M. Q. He, T. M. Leslie and J. A. Sinicropi, *Chem. Mat.*, 2002, 14, 2393-2400.
38. L. R. Dalton, P. A. Sullivan, D. H. Bale and B. C. Olbricht, *Solid-State Electronics*, 2007, 51, 1263-1277.
39. J. Wu, C. Peng, H. Xiao, S. Bo, L. Qiu, Z. Zhen and X. Liu, *Dyes Pigment.*, 2014.
40. C. C. Teng and H. T. Man, *Appl. Phys. Lett.*, 1990, 56, 1734-1736.
41. D. H. Park, C. H. Lee and W. N. Herman, *Opt. Express*, 2006, 14, 8866-8884.
42. M. A. Mortazavi, A. Knoesen, S. T. Kowel, B. G. Higgins and A. Dienes, *J. Opt. Soc. Am. B-Opt. Phys.*, 1989, 6, 733-741.
43. H. Y. Huang, G. W. Deng, J. L. Liu, J. Y. Wu, P. Si, H. J. Xu, S. H. Bo, L. Qiu, Z. Zhen and X. H. Liu, *Dyes Pigment.*, 2013, 99, 753-758.
44. Q. Q. Li, L. L. Lu, C. Zhong, J. Shi, Q. Huang, X. B. Jin, T. Y. Peng, J. G. Qin and Z. Li, *J. Phys. Chem. B*, 2009, 113, 14588-14595.
45. O. P. Kwon, M. Jazbinsek, J.-I. Seo, P.-J. Kim, E.-Y. Choi, Y. S. Lee and P. Guenter, *Dyes Pigment.*, 2010, 85, 162-170.
46. J. M. Raimundo, P. Blanchard, N. Gallego-Planas, N. Mercier, I. Ledoux-Rak, R. Hierle and J. Roncali, *J. Org. Chem.*, 2002, 67, 205-218.

second-order NLO chromophores

A' : increased electro-optic activity and stability
Br,NO$_2$: different r$_{33}$ values and solvatochromic behavior